

Transmission spectra of single crystals of MAPbI₃ hybrid perovskites near the edge of fundamental absorption

© V.E. Anikeeva^{1,2}, K.N. Boldyrev^{1,2}, O.I. Semenova³, M.N. Popova¹

¹ Institute of Spectroscopy, Russian Academy of Sciences, 108840 Troitsk, Moscow, Russia

² National Research University Higher School of Economics, 101000 Moscow, Russia

³ A.V. Rzhanov Institute of Semiconductor Physics, Siberian Branch of the Russian Academy of Sciences, 630090 Novosibirsk, Russia

e-mail: vanikeeva@hse.ru

Received July 22, 2021

Revised July 22, 2021

Accepted August 05, 2021

The paper presents the transmission spectra of hybrid perovskite MAPbI₃ single crystals near the fundamental absorption edge in a wide temperature range. The absorption coefficient α of the single crystal samples is estimated at a temperature $T = 150$ K for the light with a photon energy $E = 1.6$ eV and at $T = 40$ K for $E = 1.8$ eV. The obtained values turned out to be several orders of magnitude smaller than the values of α for thin-film samples known from the literature. A sharp shift of the fundamental absorption edge by ~ 100 meV was observed at a temperature $T_1 = 160$ K of the structural phase transition from the tetragonal to the orthorhombic phase. The temperature hysteresis of the shift of the fundamental absorption edge near T_1 was recorded, which is characteristic of a first-order phase transition.

Keywords: hybrid organometallic perovskites, MAPbI₃ single crystal, optical spectroscopy, fundamental absorption.

DOI: 10.21883/EOS.2022.01.52995.21-21

Introduction

During the last decade hybrid metalorganic perovskites (MOPs) with the chemical formula ABX₃, where A is cation of methylammonium (MA⁺ = CH₃NH₃⁺) or formamidinium (FA⁺, NH₂CH = NH₂⁺), B is metal cation (Pb, Sn), X is halogen anion (I, Br, Cl), attract many researchers from all over the world as new promising materials for use in optoelectronic devices such as thin-film solar cells (SC) [1–5], high sensitivity photodetectors [6,7], lasers, and LEDs [8]. South Korean and Swiss researchers in April 2021 reported a record value of efficiency of a single junction MOP solar cell equal to 25.6% [9]. Interest in these materials is due to a set of special optical and photoelectric characteristics that MOPs have. First of all, these are the optimal, tunable depending on the perovskite composition band gap, high absorption coefficient, non-trivial spin dynamics [10–13], light-induced structural dynamics [14–19], and long lifetimes of charge carriers [20–24].

Despite the large number of papers devoted to the study of the optical properties of MOPs, there is no full understanding of the fundamental processes that occur in hybrid perovskites when interacting with electromagnetic radiation. The main component of the solar cell is a photosensitive semiconductor layer, in which charge carriers are generated as a result of the absorption of incident radiation photons. In this regard, the determination of the value of the layer absorption coefficient is necessary for the development and optimization of SC. The available papers on the study of absorption coefficients near the band edge in MOP

mainly focus on absorption in thin films [25,26], which are used as an absorbing and/or transport layer in solar cells and other optoelectronic devices. However, it is better to study the fundamental parameters on single crystals, in particular, due to the presence of grain boundaries in polycrystalline films that scatter the incident radiation. Such losses can lead to overestimated values of the absorption coefficient.

In the present paper, the transmission spectra near the edge of fundamental absorption of large high-quality MAPbI₃ single crystals were studied.

Experiment

Synthesis of MAPbI₃ single crystals

Bulk MAPbI₃ single crystals of good quality were grown at the Rzhanov Institute of Semiconductor Physics of the Siberian Branch of the of Russian Academy of Science according to the method described in detail in the papers [27,28]. For the synthesis of MAPbI₃ polycrystalline powder, a reaction between two precursors was used: MAI (methyl ammonium iodide) and PbI₂ (lead iodide). The resulting MAPbI₃ powder was dissolved in hydroiodic acid HI until saturation at 65°C, then the solution was placed in a closed reaction chamber with a precision temperature decreasing from 65°C to 21°C with increments of 0.1°C per hour. Within 10–12 days black shiny single crystals grew up to 1 cm in size.

The composition and structure of the grown single crystals were verified by X-ray diffraction and X-ray photoelectron spectroscopy. The good structural quality of the single crystal surface was demonstrated by the RHEED method (reflection high-energy electron diffraction) [29].

Transmission spectra measurements in the near infrared and visible ranges

The transmission spectra were measured on a unique experimental setup, including Bruker IFS 125HR high-resolution Fourier spectrometer and Cryomech ST 403 closed cycle cryostat. A single crystal 1.4 mm thick was fixed on a copper substrate using silver paste. Then the substrate was attached to the copper finger of the cryostat in such a way that the natural face of the crystal (100) was directed perpendicular to the incident radiation. The temperature of the copper finger could vary from 5 to 350 K. Globar was used as a radiation source. The radiation that passed through the crystal was recorded by a silicon detector operating in the range of 8500–20000 cm⁻¹. The spectra were obtained with a resolution up to 2 cm⁻¹.

Results and discussion

The transmission spectra of the MAPbI₃ single crystal in the frequency range of 11695–14518 cm⁻¹ are shown in Fig. 1. As the temperature is lowered from 340 K to 250 K, the absorption edge slightly shifts, first to the blue, and then from 250 K to 160 K — back to the red region of the spectrum. In typical inorganic semiconductors, such as Si, Ge, or GaAs, the band gap edge shifts to higher energies region with temperature decreasing, according to Varshni's empirical relation:

$$E_g = E_0 - \frac{\alpha T^2}{T + \beta}, \quad (1)$$

where E_0 is the band gap width at $T = 0$ K, α , β are constants [30]. Such unusual behavior for MAPbI₃ was also observed in previous papers [31–33]. In paper [32], it was supposed that it is associated with the energy increasing of the valence band maximum with temperature decrease.

The structural phase transition at temperature $T_2 = 330$ K from the cubic to the tetragonal phase is not marked by any features on the temperature dependence of the position of the fundamental absorption edge. At the temperature T_1 of the structural phase transition from the tetragonal to the orthorhombic phase, a dramatic shift of the fundamental absorption boundary by 0.11 eV, i.e. from 1.63 to 1.52 eV, is observed. Such a difference of about 100 meV between the energies of the band edge in two structural phases was observed earlier in papers [25,34] and was explained by the tilt effect of the [PbI₆]⁴⁻ octahedrons upon transition from one phase to another [35].

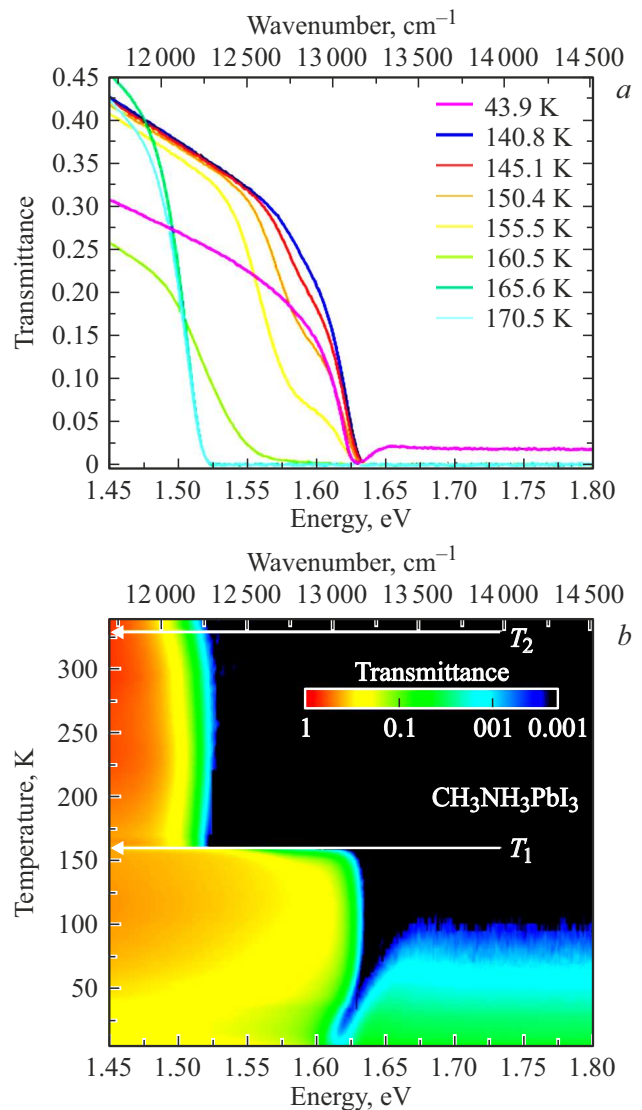


Figure 1. Transmission spectra of MAPbI₃ single crystal near the fundamental absorption edge at temperature of 44 K and in the region of low-temperature structural phase transition at temperatures from 140 K to 170 K (a) and presented as intensity map in the axes frequency–temperature (b). Sample thickness is 1.4 mm. The white horizontal lines mark the temperatures of the structural phase transitions T_1 and T_2 .

The transmission spectra at low temperatures show a narrow exciton band with an absorption maximum at about 1.62 eV at 5 K, which agrees with the results of earlier studies. For example, in the paper [26], where MAPbI₃ polycrystalline films were studied, the peak at 1.64 eV in the optical density spectra at a temperature of 4.2 K was also explained by exciton transition. The position of the exciton peak 1.633 eV ($T = 4.2$ K) was found from the reflection spectra of MAPbI₃ single crystal using the Kramers–Kronig relation [36]. The exact calculation of the absorption coefficient of thin-film perovskite CH₃NH₃PbI₃ using the reflection and transmission spectra gave a value of

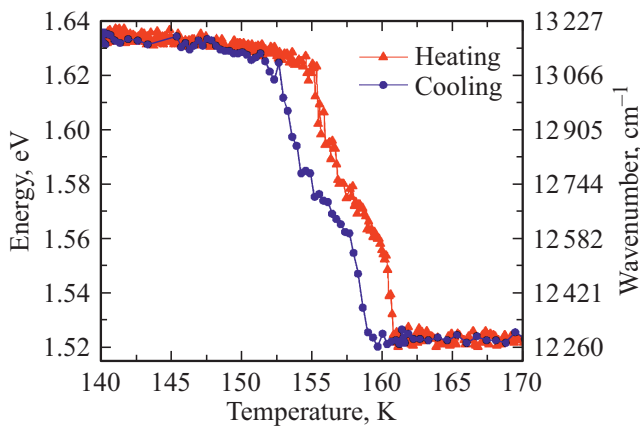


Figure 2. Temperature dependences of the position of the absorption edge of the MAPbI₃ single crystal, obtained by cooling (blue circles) and heating (red triangles) of the sample.

1.640 eV ($T = 4.2$ K) for energy of the exciton peak [25]. Further theoretical modeling of absorption spectra allowed the authors [25] to separate the contributions from states of continuum and bound electron-hole pairs (exciton states) and find the exciton binding energy $E_{\text{ex}} = 20 \pm 2$ meV for the low-temperature orthorhombic phase. In the present paper, E_{ex} could not be determined because of the saturation of the transmission spectra of thick single-crystal sample.

In paper [25], the absorption coefficient α in the range from 1.5 to 2.0 eV was obtained from the reflectance (R) and the transmittance (Tr) according to the expression:

$$\alpha = -\frac{1}{d} \ln \left(\frac{Tr}{1-R} \right), \quad (2)$$

where d is sample thickness. The sequence of absorption spectra in the temperature range of 4–295 K with increment of 5–10 K (Fig. 3 in the Supplementary Information to the paper [25]) clearly shows a sharp shift of the band edge during the phase transition from orthorhombic to tetragonal structure, the formation of exciton peak with temperature decreasing, and the coexistence of two phases in the temperature range of 140–170 K. Our data are in qualitative agreement with the data [25], however, there are significant quantitative discrepancies. In particular, at 155 K, the residual peak at the energy ~ 1.60 eV of the high-temperature phase with the maximum absorption coefficient $\alpha_m = 10^4 \text{ cm}^{-1}$ was observed in [25] on the high-frequency side of the exciton peak belonging to the low-temperature phase. We also observe this peak (Fig. 1, *a*), however, the maximum absorption coefficient is $\alpha_m = 18 \text{ cm}^{-1}$, but not 10^4 cm^{-1} . In high temperature tetragonal phase, the transmission spectra of the single crystal 1.4 mm thick studied in this work are saturated above the absorption edge. Below the phase transition temperature in the low-temperature orthorhombic phase the sample is partially transparent above the exciton peak. Such the absorption

coefficient decreasing was also registered in [25]. In particular, it was reported that $\alpha(170 \text{ K}) = 3.2 \cdot 10^4 \text{ cm}^{-1}$, while $\alpha(40 \text{ K}) = 2.9 \cdot 10^4 \text{ cm}^{-1}$ at energy of 1.8 eV (Fig. 3 in the Supplementary Information to paper [25]). At this wavelength (1.8 eV corresponds to $\lambda = 689 \text{ nm}$) our 1.4 mm thick sample is completely opaque at 170 K. It would remain completely opaque even at 4 K if the absorption coefficient was $\sim 10^4 \text{ cm}^{-1}$ according to [25]. The estimate of the absorption coefficient for the transmission spectra of our CH₃NH₃PbI₃ single crystal gives $\alpha(40 \text{ K}, \lambda = 689 \text{ nm}) = 28 \text{ cm}^{-1}$. Thus, the obtained experimental data for single crystal of good optical quality convincingly show that for the thin films, studied in [25], some losses (for example, scattering) were not taken into account, which led to overestimated values of the intrinsic absorption coefficient of CH₃NH₃PbI₃ near the fundamental absorption edge.

Figure 2 shows the temperature dependences of the position of the fundamental absorption edge near the low-temperature phase transition, obtained from the transmission spectra of CH₃NH₃PbI₃ single crystal 1.4 mm thick and recorded during cooling and heating of the sample. The position of the absorption edge was determined as the value of the maximum of the derivative dTr/dE . A noticeable temperature hysteresis with a width $\Delta T = 2$ K is seen, which confirms the first-order phase transition. The complex form of the dependence is due to the fact that the spectra have complex structure due to the coexistence of two structural phases in the transition region.

Conclusion

The optical transmission of a good-quality single crystal of a hybrid organometallic perovskite, methylammonium lead iodide MAPbI₃ was measured near the fundamental absorption edge, in a wide temperature range (5–330 K). A shift of the band edge of about 100 meV was observed during the structural phase transition between the tetragonal and orthorhombic phases, as well as the formation of an exciton peak upon temperature decreasing. The fact that the transition is of the first order is confirmed by the presence of hysteresis. The absorption coefficients α (1.6 eV, 150 K) and α (1.8 eV, 40 K) were estimated. Their values are almost by three orders of magnitude lower than the values obtained on thin MAPbI₃ films [25]. This may be due to the fact that the films have losses due to scattering, for example, at grain boundaries, and they are not taken into account. The true values of the absorption coefficient in the substance should be measured on single crystals of good quality.

Funding

The publication was prepared as a result of research within the framework of the Academic Fund Program at the HSE University in 2020–2021 (№ 21-04-016). Crystal growth was performed by O.I.S. and supported by the

Ministry of Science and Higher Education of Russia (Grant 0306-2019-0015).

Conflict of interest

The authors declare that they have no conflict of interest.

References

- [1] National Renewable Energy Laboratory. Best Research-Cell Efficiency Chart [Electronic source]. URL: <https://www.nrel.gov/pv/cell-efficiency.html>
- [2] W.S. Yang, B.-W. Park, E.H. Jung, N.J. Jeon, Y.C. Kim, D.U. Lee, S.S. Shin, J. Seo, E.K. Kim, J.H. Noh, S.I. Seok. *Science*, **356** (6345), 1376 (2017). DOI: 10.1126/science.aan2301
- [3] J.-P. Correa-Baena, A. Abate, M. Saliba, W. Tress, T.J. Jacobsson, M. Grätzel, A. Hagfeldt. *Energy Environ. Sci.*, **10** (3), 710 (2017). DOI: 10.1039/C6EE03397K
- [4] H. Tan, A. Jain, O. Voznyy, X. Lan, F.P.G. De Arquer, J.Z. Fan, R. Quintero-Bermudez, M. Yuan, B. Zhang, Y. Zhao, F. Fan, P. Li, L.N. Quan, Y. Zhao, Z.-H. Lu, Z. Yang, S. Hoogland, E.H. Sargent. *Science*, **355** (6326), 722 (2017). DOI: 10.1126/science.aai9081
- [5] S. Bai, P. Da, C. Li, Z. Wang, Z. Yuan, F. Fu, M. Kawecki, X. Liu, N. Sakai, J.T.-W. Wang, S. Huettner, S. Buecheler, M. Fahlman, F. Gao, H.J. Snaith. *Nature*, **571**, 245 (2019). DOI: 10.1038/s41586-019-1357-2
- [6] D. Yu, F. Cao, Y. Gu, Z. Han, J. Liu, B. Huang, X. Xu, H. Zeng. *Nano Res.*, **14** (4), 1210 (2021). DOI: 10.1007/s12274-020-3174-1
- [7] J. Miao, F. Zhang. *J. Mater. Chem. C.*, **7**, 1741 (2019). DOI: 10.1039/C8TC06089D
- [8] P. Du, L. Gao, J. Tang. *Front. Optoelectron.*, **13** (3), 235 (2020). DOI: 10.1007/s12200-020-1042-y
- [9] J. Jeong, M. Kim, J. Seo, H. Lu, P. Ahlawat, A. Mishra, Y. Yang, M. Hope, F. Eickemeyer, M. Kim, Y. Yoon, I. Choi, B. Darwich, S. Choi, Y. Jo, J. Lee, B. Walker, S. Zakeeruddin, L. Emsley, U. Rothlisberger, A. Hagfeldt, D. Kim, M. Grätzel, J. Kim. *Nature*, **592**, 381 (2021). DOI: 10.1038/s41586-021-03406-5
- [10] D. Giovanni, H. Ma, J. Chua, M. Grätzel, R. Ramesh, S. Mhaisalkar, N. Mathews, T.C. Sum. *Nano Lett.*, **15** (3), 1553 (2015). DOI: 10.1021/nl5039314
- [11] F. Zheng, L.Z. Tan, S. Liu, A.M. Rappe. *Nano Lett.*, **15** (12), 7794 (2015). DOI: 10.1021/acs.nanolett.5b01854
- [12] C. Zhang, D. Sun, Z.V. Vardeny. *Novel Spin Physics in Organic–Inorganic Perovskites*. In: *Halide Perovskites: Photovoltaics, Light Emitting Devices, and Beyond*, ed. by T.-C. Sum, N. Mathews (Weinheim: Wiley-VCH Verlag GmbH & Co. KGaA, Germany, 2018), p. 249–271.
- [13] D. Niesner, M. Hauck, S. Shrestha, I. Levchuk, G.J. Matt, A. Osvet, M. Batentschuk, C. Brabec, H.B. Weber, T. Fauster. *PNAS*, **115** (38), 9509 (2018). DOI: 10.1073/pnas.1805422115
- [14] R. Gottesman, L. Gouda, B.S. Kalanoor, E. Haltzi, S. Tirosh, E. Rosh-Hodesh, Y. Tischler, A. Zaban, C. Quarti, E. Mosconi, F. De Angelis. *J. Phys. Chem. Lett.* **6** (12), 2332 (2015). DOI: 10.1021/acs.jpcclett.5b00994
- [15] H. Zhu, K. Miyata, Y. Fu, J. Wang, P.P. Joshi, D. Niesner, K.W. Williams, S. Jin, X.-Y. Zhu. *Science*, **353** (6306), 1409 (2016). DOI: 10.1126/science.aaf9570
- [16] X. Wu, L.Z. Tan, X. Shen, T. Hu, K. Miyata, M.T. Trinh, R. Li, R. Coffee, S. Liu, D.A. Egger, I. Makasyuk, Q. Zheng, A. Fry, J.S. Robinson, M.D. Smith, B. Guzelturk, H.I. Karunadasa, X. Wang, X. Zhu, L. Kronik, A.M. Rappe, A.M. Lindenberg. *Sci. Adv.* **3** (7), e1602388 (2017). DOI: 10.1126/sciadv.1602388
- [17] H. Tsai, R. Asadpour, J.-C. Blancon, C.C. Stoumpos, O. Durand, J.W. Strzalka, B. Chen, R. Verduzco, P.M. Ajayan, S. Tretiak, J. Even, M.A. Alam, M.G. Kanatzidis, W. Nie, A.D. Mohite. *Science*, **360** (6384), 67 (2018). DOI: 10.1126/science.aap8671
- [18] H.-C. Hsu, B.-C. Huang, S.-C. Chin, C.-R. Hsing, D.-L. Nguyen, M. Schnedler, R. Sankar, R.E. Dunin-Borkowski, C.-M. Wei, C.-W. Chen, P. Ebert, Y.-P. Chiu. *ACS Nano*, **13** (4), 4402 (2019). DOI: 10.1021/acsnano.8b09645
- [19] J. Xue, D. Yang, B. Cai, X. Xu, J. Wang, H. Ma, X. Yu, G. Yuan, Y. Zou, J. Song, H. Zeng. *Adv. Funct. Mater.*, **29** (13), 1807922 (2019). DOI: 10.1002/adfm.201807922
- [20] C. Wehrenfennig, G.E. Eperon, M.B. Johnston, H.J. Snaith, L.M. Herz. *Adv. Mater.*, **26** (10), 1584 (2014). DOI: 10.1002/adma.201305172
- [21] D. Shi, V. Adinolfi, R. Comin, M. Yuan, E. Alarousu, A. Buin, Y. Chen, S. Hoogland, A. Rothenberger, K. Katsiev, Y. Losovyj, X. Zhang, P.A. Dowben, O.F. Mohammed, E.H. Sargent, O.M. Bakr. *Science*, **347** (6221), 519 (2015). DOI: 10.1126/science.aaa2725
- [22] Q. Dong, Y. Fang, Y. Shao, P. Mulligan, J. Qiu, L. Cao, J. Huang. *Science*, **347** (6225), 967 (2015). DOI: 10.1126/science.aaa5760
- [23] Y. Bi, E.M. Hutter, Y. Fang, Q. Dong, J. Huang, T.J. Savenije. *J. Phys. Chem. Lett.*, **7** (5), 923 (2016). DOI: 10.1021/acs.jpcclett.6b00269
- [24] E. Alarousu, A.M. El-Zohry, J. Yin, A.A. Zhumekenov, C. Yang, E. Alhabshi, I. Gereige, A. AlSaggaf, A.V. Malko, O.M. Bakr, O.F. Mohammed. *J. Phys. Chem. Lett.*, **8** (18), 4386 (2017). DOI: 10.1021/acs.jpcclett.7b01922
- [25] C.L. Davies, M.R. Filip, J.B. Patel, T.W. Crothers, C. Verdi, A.D. Wrigth, R.L. Milot, F. Giustino, M.B. Johnston, L.M. Herz. *Nat. Commun.*, **9**, 293 (2018). DOI: 10.1038/s41467-017-02670-2
- [26] V. D’Innocenzo, G. Grancini, M.J.P. Alcocer, A.R.S. Kandada, S.D. Stranks, M.M. Lee, G. Lanzani, H.J. Snaith, A. Petrozza. *Nat. Commun.*, **5**, 3586 (2014). DOI: 10.1038/ncomms4586
- [27] O.I. Semenova, E.S. Yudanova, N.A. Yeryukov, Y.A. Zhivodkov, T.S. Shamirzaev, E.A. Maximovskiy, S.A. Gromilov, I.B. Troitskaia. *J. Cryst. Growth.*, **462** (15), 45 (2017). DOI: 10.1016/j.jcrysgro.2017.01.019
- [28] E.S. Yudanova, T.A. Duda, O.E. Tereshchenko, O.I. Semenova. *J. Struct. Chem.*, **58**, 1567 (2017). DOI: 10.1134/S0022476617080133
- [29] V.E. Anikeeva, O.I. Semenova, O.E. Tereshchenko. *J. Phys.: Conf. Ser.*, **1124**, P.041008 (2018). DOI: 10.1088/1742-6596/1124/4/041008
- [30] Y.P. Varshni. *Physica*, **34** (1), 149 (1967). DOI: 10.1016/0031-8914(67)90062-6
- [31] W. Huang, S. Yue, Y. Liu, L. Zhu, P. Jin, Q. Wu, Y. Zhang, Y. Chen, K. Liu, P. Liang, S. Qu, Z. Wang, Y. Chen. *ACS Photonics*, **5** (4), 1583 (2018). DOI: 10.1021/acsphotonics.8b00033

- [32] B.J. Foley, D.L. Marlowe, K. Sun, W.A. Saidi, L. Scudiero, M.C. Gupta, J.J. Choi. *Appl. Phys. Lett.*, **106**, 243904 (2015). DOI: 10.1063/1.4922804
- [33] C. Quarti, E. Mosconi, J.M. Ball, V. D’Innocenzo, C. Tao, S. Pathak, H.J. Snaith, A. Petrozza, F. De Angelis. *Energy Environ. Sci.*, **9** (1), 155 (2016). DOI: 10.1039/C5EE02925B
- [34] R.L. Milot, G.E. Eperon, H.J. Snaith, M.B. Johnston, L.M. Herz. *Adv. Func. Mater.*, **25** (39) 6218 (2015). DOI: 10.1002/adfm.201502340
- [35] C. Katan, L. Pedesseau, M. Kepenekian, A. Rolland, J. Even. *J. Mater. Chem. A.*, **3** (17), 9232 (2015). DOI: 10.1039/C4TA06418F
- [36] M. Hirasawa, T. Ishihara, T. Goto. *J. Phys. Soc. Jpn.*, **63** (10), 3870 (1994). DOI: 10.1143/JPSJ.63.3870